AMERICAN SOCIETY FOR MICROBIOLOGY | Antimicrobial Agents and Chemotherapy®

Complex Interplay between Sphingolipid and Sterol Metabolism Revealed by Perturbations to the *Leishmania* Metabolome Caused by Miltefosine

Emily G. Armitage,[a,b,c] Amjed Q. I. Alqaisi,[d,e] Joanna Godzien,[a] Imanol Peña,[b] Alison J. Mbekeani,[d] Vanesa Alonso-Herranz,[a] Ángeles López-Gonzálvez,[a] Julio Martín,[b] Raquel Gabarro,[b] Paul W. Denny,[d] Michael P. Barrett,[c] Coral Barbas[a]

[a]Centre for Metabolomics and Bioanalysis (CEMBIO), Facultad de Farmacia, Universidad CEU San Pablo, Campus Montepríncipe, Boadilla del Monte, Madrid, Spain

[b]GSK I+D Diseases of the Developing World (DDW), Parque Tecnológico de Madrid, Tres Cantos, Madrid, Spain

[c]Wellcome Centre for Molecular Parasitology, Institute of Infection, Immunity and Inflammation, College of Medical, Veterinary and Life Sciences & Glasgow Polyomics, University of Glasgow, Glasgow, United Kingdom

[d]Department of Biosciences, Durham University, Lower Mountjoy, Durham, United Kingdom

[e]University of Baghdad, College of Science, Biology Department, Baghdad, Iraq

ABSTRACT With the World Health Organization reporting over 30,000 deaths and 200,000 to 400,000 new cases annually, visceral leishmaniasis is a serious disease affecting some of the world's poorest people. As drug resistance continues to rise, there is a huge unmet need to improve treatment. Miltefosine remains one of the main treatments for leishmaniasis, yet its mode of action (MoA) is still unknown. Understanding the MoA of this drug and parasite response to treatment could help pave the way for new and more successful treatments for leishmaniasis. A novel method has been devised to study the metabolome and lipidome of *Leishmania donovani* axenic amastigotes treated with miltefosine. Miltefosine caused a dramatic decrease in many membrane phospholipids (PLs), in addition to amino acid pools, while sphingolipids (SLs) and sterols increased. *Leishmania major* promastigotes devoid of SL biosynthesis through loss of the serine palmitoyl transferase gene (ΔLCB2) were 3-fold less sensitive to miltefosine than wild-type (WT) parasites. Changes in the metabolome and lipidome of miltefosine-treated *L. major* mirrored those of *L. donovani*. A lack of SLs in the ΔLCB2 mutant was matched by substantial alterations in sterol content. Together, these data indicate that SLs and ergosterol are important for miltefosine sensitivity and, perhaps, MoA.

KEYWORDS *Leishmania*, lipid metabolism, mechanisms of action, metabolomics, miltefosine

Infectious diseases continue to cause great morbidity and mortality worldwide (1). New drugs are required and will need to be continuously replenished as resistance to antimicrobials increases. Understanding the mode of action (MoA) of currently available treatments against microbial diseases offers a means to highlight targets for new treatments. Metabolomics plays an important role in this discovery and development of new medicines for infectious diseases (1).

The leishmaniases are a spectrum of neglected tropical diseases caused by protozoa of the genus *Leishmania*. Individual species provoke different clinical manifestations, including visceral leishmaniasis caused by *Leishmania donovani* and *Leishmania infantum* (2) which is fatal if not treated. Existing therapeutic options are limited (3), so the search for alternative therapies continues. Two key developmental stages of *Leishmania* are used for *in vitro* studies of drug MoA: amastigotes and, more commonly, promastigotes. Promastigotes are the form found in the sand fly vector, while amastigotes exist

Received 12 October 2017 **Returned for modification** 20 November 2017 **Accepted** 21 January 2018

Accepted manuscript posted online 20 February 2018

Citation Armitage EG, Alqaisi AQI, Godzien J, Peña I, Mbekeani AJ, Alonso-Herranz V, López-Gonzálvez Á, Martín J, Gabarro R, Denny PW, Barrett MP, Barbas C. 2018. Complex interplay between sphingolipid and sterol metabolism revealed by perturbations to the *Leishmania* metabolome caused by miltefosine. Antimicrob Agents Chemother 62:e02095-17. https://doi.org/10.1128/AAC.02095-17.

Address correspondence to Paul W. Denny, p.w.denny@durham.ac.uk, Michael P. Barrett, Michael.Barrett@glasgow.ac.uk, or Coral Barbas, cbarbas@ceu.es.

in the mammalian host. The development of axenic cultures having physiological similarity to the macrophage resident forms in mammalian infections has made it possible to study amastigotes *in vitro* (2).

Metabolomics seeks comprehensive measurements of small molecules in a given system. However, the dynamic range in abundance and broad physicochemical diversity of metabolites is such that a single analytical platform is lacking. Here, a combined liquid chromatography-mass spectrometry (LC-MS) and capillary electrophoresis-mass spectrometry (CE-MS) approach was used to increase coverage of the *Leishmania* metabolome and applied to study the MoA of miltefosine, the first drug approved for oral treatment of leishmaniasis. Metabolomics has proven useful in drug MoA studies for *Leishmania* promastigotes (4–13) but so far not for *L. donovani* amastigotes. *Leishmania mexicana* amastigotes were recently studied using metabolomics to show that amastigote differentiation is associated with the induction of a distinct stringent metabolic state (14) in both lesion-derived and *in vitro* differentiated amastigotes.

Several suggestions have been made regarding the antileishmanial action of miltefosine, occurring either via induction of apoptosis-like death (15, 16) or disruption of metabolite transport (4, 17, 18). The uptake of miltefosine in *Leishmania* spp. is dependent on transmembrane lipid transporters, most notably the flippase LdMT and its accessory protein, LdRos, which are commonly lost with the selection of resistance (19). More recently, using cosmid-based functional cloning coupled with next-generation sequencing, genes involved in ergosterol biosynthesis and phospholipid (PL) translocation were suggested to contribute to resistance in *L. infantum* (20).

Metabolomic analyses of miltefosine-treated *L. infantum* strains showed a general depletion of intracellular metabolites (6), and similar studies in other *Leishmania* spp. demonstrated lipid remodelling (21–24). Biochemical modifications to different lipid classes have been reported in the membranes of miltefosine-treated *L. donovani* promastigotes (22). In addition to diminishing phosphatidylcholine (PC), miltefosine was found to double sterol composition as well (22). The effects of miltefosine treatment on lipid metabolism in promastigotes of *L. infantum* (6) have also been observed using metabolomics, although only lipid class rather than individual lipid species was resolved. Combining CE-MS to analyze polar and ionic metabolites and reversed-phase LC-MS to reveal specific lipidomic changes in *L. donovani* has allowed a more detailed analysis into the MoA in axenic amastigotes presented herein.

Substantial changes in sphingolipid (SL) and sterol metabolism were revealed in miltefosine-treated *L. donovani* promastigotes. SLs were first reported in *L. donovani* more than 20 years ago (25), and along with sterols, have since received attention in many species (26–28). *Leishmania* spp. obtain SLs via salvage or *de novo* synthesis (29), and they play important roles in differentiation, replication, trafficking, and virulence (29). The prominent, and most studied, SL identified is inositol phosphoceramide (IPC), although *Leishmania* spp. are believed to exhibit a complete and functional SL pathway involving both biosynthesis and degradation (28, 30). A more comprehensive analysis of different SLs may identify other key targets of SL metabolism for therapy. To study the viability of *Leishmania* spp. without SL synthesis, a mutant was created by deletion of the gene encoding the essential catalytic subunit of the serine palmitoyltransferase (ΔLCB2), the first and rate-limiting step in SL biosynthesis (28, 31). Surprisingly, this mutant was viable, indicating a dispensable role for SLs in *Leishmania* spp., unlike in the related parasite *Trypanosoma brucei* (32). It was suggested that the sterol composition of the *Leishmania* plasma membrane, where ergosterol replaces cholesterol as the primary membrane sterol, could enable this (32). Here, perturbations to *Leishmania* SL and sterol metabolism on miltefosine treatment are described, the interplay between these metabolite families is considered, and the role sterols play in drug sensitivity is proposed.

RESULTS AND DISCUSSION

In order to define the optimal protocol for sampling/quenching/extracting/analyzing metabolites from *L. donovani* axenic amastigotes, a method was developed as

described below and further in the supplemental material (File S1). The extraction procedure was optimized such that LC-MS and CE-MS analyses could be performed from single samples of as few as 1×10^7 parasites (Fig. S1). For *L. donovani*, samples were treated with 4.47 μM (the observed 50% effective concentration [EC_{50}] at 72 h, consistent with the literature [33]) or 13.41 μM (three times the observed EC_{50} at 72 h) miltefosine and harvested after 5 h or 24 h of exposure to observe the initial effects of the drug. For *L. major*, samples were treated with 10 μM or 30 μM miltefosine and harvested after 5 h of exposure. Dimethyl sulfoxide (DMSO) controls were prepared alongside treated samples at each time point for both species. The results from method development stages are detailed in the supplemental material: a comparison of methanol extraction and a more comprehensive extraction for lipidomics using LC-MS is shown in Fig. S2, profiles obtained using LC-MS and CE-MS analysis of different extractions are shown in Fig. S3, and the final optimized dual extraction procedure to obtain different extracts for LC-MS and CE-MS analysis from single samples is shown in Fig. S4.

Metabolomic determination of *Leishmania* response to miltefosine. With the exception of the aforementioned work on *L. mexicana* amastigotes (14), the few studies on drug MoA in *Leishmania* spp. have focused on the promastigote form (2–10). The aim of this research was to explore effects on metabolism of miltefosine in *L. donovani* axenic amastigotes and, as a result of these findings, in *L. major* promastigotes.

After verification of quality (Fig. S5), data were divided into separate sets, and differences between treated and untreated parasites were identified. Around 20 metabolites, including the drug itself, were detected only in the treated samples. These features (listed on the "Miltefosine related metabolites" tab in the supplemental tables file) were all found to elute with the drug and therefore were most likely enhanced by ionization of the drug. These could not be identified as endogenous lipids and were therefore assumed to be mass spectrometry derivatives of the drug itself. All were removed prior to multivariate analysis to avoid separation based on the presence or absence of drug alone. Identification was performed for metabolite features found to increase/decrease with treatment after 5 or 24 h of exposure, determined by a P value of <0.05 (Student's two-tailed t test, $n = 6$ per group) and a fold change of ± 1.5 calculated for at least one of the comparisons made. Identification of metabolites found by CE-MS was confirmed by injection of authentic standards (as detailed in Table S1). Lipids detected using LC-MS were annotated considering chemical properties and elution order. Miltefosine treatment affected different metabolic classes, and the possible impact on MoA is discussed below, based on data presented in the supplemental tables, a description for which is given in the supplemental material.

***L. donovani* axenic amastigotes.** Miltefosine has been proposed to affect the transport of different metabolites (4, 17, 18). Consistent with previous literature (6), miltefosine induced decreases in the majority of internal metabolites detected by CE-MS, as shown in Table 1, which could be associated with impaired uptake. Figure 1 shows the abundances of metabolites associated with arginine metabolism detected in this study. Arginine is a precursor to polyamine biosynthesis and a protein building block. Its intracellular concentration is controlled by dedicated sensory protein transporters (10, 18), which have been suggested to be targets of miltefosine (4). Arginase, which catalyzes the hydrolysis of arginine to ornithine, also contributes to the intracellular concentration of arginine. The coordinated decrease in arginine and ornithine may indicate a reduction in precursor levels (through blocking arginine transport), a notion consistent with previously reported literature (34, 35). Another metabolite that shares the same mass but has a distinct migration time to citrulline was identified as argininic acid, which is considered an endpoint of arginine metabolism previously found in different *Leishmania* species, including *L. donovani* (36). Its concentration was substantially reduced with treatment at both time points and doses (up to 3-fold) in this research.

TABLE 1 Metabolites identified in *Leishmania donovani* axenic amastigotes and significantly affected by miltefosine

Metabolite (MSI level 1)[a]	*m/z*	Migration time (min)	5 h exposure[b]				24 h exposure[b]			
			P value		Fold change		*P* value		Fold change	
			LD	HD	LD	HD	LD	HD	LD	HD
Acetyl-carnitine	204.1232	13.93	3.71E-02	2.30E-05	1.1	1.5	1.28E-03	4.37E-04	1.5	2.4
Adenosine	268.1042	15.23	NS	NS			8.03E-04	4.22E-04	3.7	57.3
Alanine	90.0552	13.95	6.86E-03	2.47E-03	1.3	1.4	2.49E-05	1.33E-06	1.7	5.4
Argininic acid	176.1032	14.19	1.32E-02	2.57E-04	1.2	1.6	9.30E-08	2.85E-08	2.8	6.8
Asparagine	133.0612	15.89	9.15E-03	2.60E-02	1.4	1.3	NS	4.30E-02		1.7
Betaine	118.0862	17.09	1.49E-02	NS	1.2		NS	4.51E-03		1.2
Choline	104.1072	10.92	1.35E-05	NS	1.5		3.24E-04	NS	1.4	
Citrulline	176.1032	16.68	9.08E-03	NS	1.3		1.47E-06	1.39E-05	1.6	1.4
Isoleucine	132.1022	15.52	2.56E-02	1.83E-04	1.3	3.0	1.39E-06	6.56E-06	2.1	4.2
Leucine	132.1022	15.65	4.61E-02	5.08E-03	1.3	1.8	3.91E-03	4.15E-04	1.9	3.2
Lysine	147.1122	11.14	5.50E-04	5.73E-05	1.6	2.7	1.29E-05	1.24E-06	2.1	2.9
Pipecolic acid	130.0862	15.62	6.08E-04	5.05E-04	1.8	1.8	3.78E-03	9.20E-07	1.3	4.3
Valine	118.0862	15.28	2.95E-03	5.84E-06	1.3	2.5	4.36E-06	3.20E-07	2.1	3.6
Glutamic acid	148.0682	16.51	NS	3.22E-05	1.1	1.3	4.18E-04	2.46E-09	1.2	4.7
Aspartic acid	134.0452	17.27	NS	NS			6.56E-03	1.64E-07	1.2	3.0
Creatine	132.0772	13.79	NS	NS			2.42E-04	1.21E-04	1.9	2.5
Histidine	156.0772	11.72	NS	2.49E-03		1.8	1.85E-06	1.55E-06	2.3	11.0
Arginine	175.1192	11.44	NS	9.87E-03		1.3	2.10E-08	1.18E-09	2.4	6.0
Proline	116.0702	11.04	NS	1.39E-02		2.1	5.35E-06	6.07E-06	4.0	40.2
Ornithine	133.0972	11.06	NS	1.45E-02		2.0	7.53E-06	7.94E-06	4.2	34.6
Adenine	136.0612	12.12	NS	NS			4.06E-03	1.90E-03	4.1	17.5
Thiamine	265.1122	10.67	NS	2.19E-02		1.6	1.13E-02	3.73E-02	2.0	2.0
Methionine	150.0592	16.17	NS	NS			4.43E-05	7.76E-05	2.2	6.4
S-Adenosylhomocysteine	385.1292	13.73	NS	3.87E-02		1.5	2.68E-03	7.44E-05	1.8	NC
Trans-4-hydroxyproline	132.0652	17.99	NS	NS			1.09E-05	1.25E-05	1.3	1.4
Phenylalanine	166.0872	16.65	NS	NS			6.82E-03	8.71E-03	1.4	2.0
Carnitine	162.1122	13.30	NS	2.15E-03		1.2	9.26E-08	1.93E-08	1.5	3.7

[a]Metabolites identified in CE-MS analysis of *Leishmania donovani* axenic amastigotes as being significantly affected by miltefosine treatment in different doses/time points. All identifications have been determined at MSI (metabolomics standards initiative) level 1, as defined by the analysis of authentic standards.

[b]Calculated *P* values (Student's two-tailed *t* test [$n = 6$ per group]) and fold changes are shown for the lower dose (LD; 4.47 μM) and higher dose (HD; 13.41 μM) versus the untreated samples at the respective time point. Where *P* values were not significant (NS; $P > 0.05$), there were no fold changes to report. Fold changes are absolute; all are decreases except those highlighted in gray, which are calculated increases with miltefosine with respect to the untreated controls.

While data from CE-MS largely confirmed observations in the literature, the approach here has given a finer-grained view of the effect of miltefosine on lipids. *Leishmania* membrane lipids differ substantially in composition and function from those in mammals, making them important for viability and virulence as well as potential drug targets (29). Lipids have been analyzed previously in *L. donovani* (7, 22, 29, 37), as have changes in lipid metabolism connected to miltefosine treatment (21–23, 38, 39). Here, we demonstrate more detail on individual lipid species than has previously been reported.

In *L. infantum*, miltefosine was reported to alter 10% of the metabolome, purportedly due to compromised outer membrane integrity leading to lysis (6). Here, a general decrease in membrane PL abundance was observed in *L. donovani* axenic amastigotes (see Tables S2 to S4 for specific lipids). Miltefosine was reported by Zufferey et al. to inhibit PC biosynthesis, diminishing levels in *L. donovani* promastigotes leading to growth arrest (21). Phospholipase D activity was unaffected by the drug; hence, inhibition of the choline transporter was proposed to underlie the reduction in PC biosynthesis (21). A number of PCs and other PLs were found diminished in this study as well (Table S2).

Other considerable effects of treatment observed were increases in sterols and, to an even greater extent, SLs. To investigate this further, all filtered LC-MS data were scanned to identify peaks identifiable as SLs (even if the relative levels in treated and untreated parasites were not statistically different). Figure 2 shows the trends observed in SLs, where data are plotted for untreated parasites and parasites treated with the lowest dose of miltefosine at 24 h. A dramatic and significant (5-fold) increase in

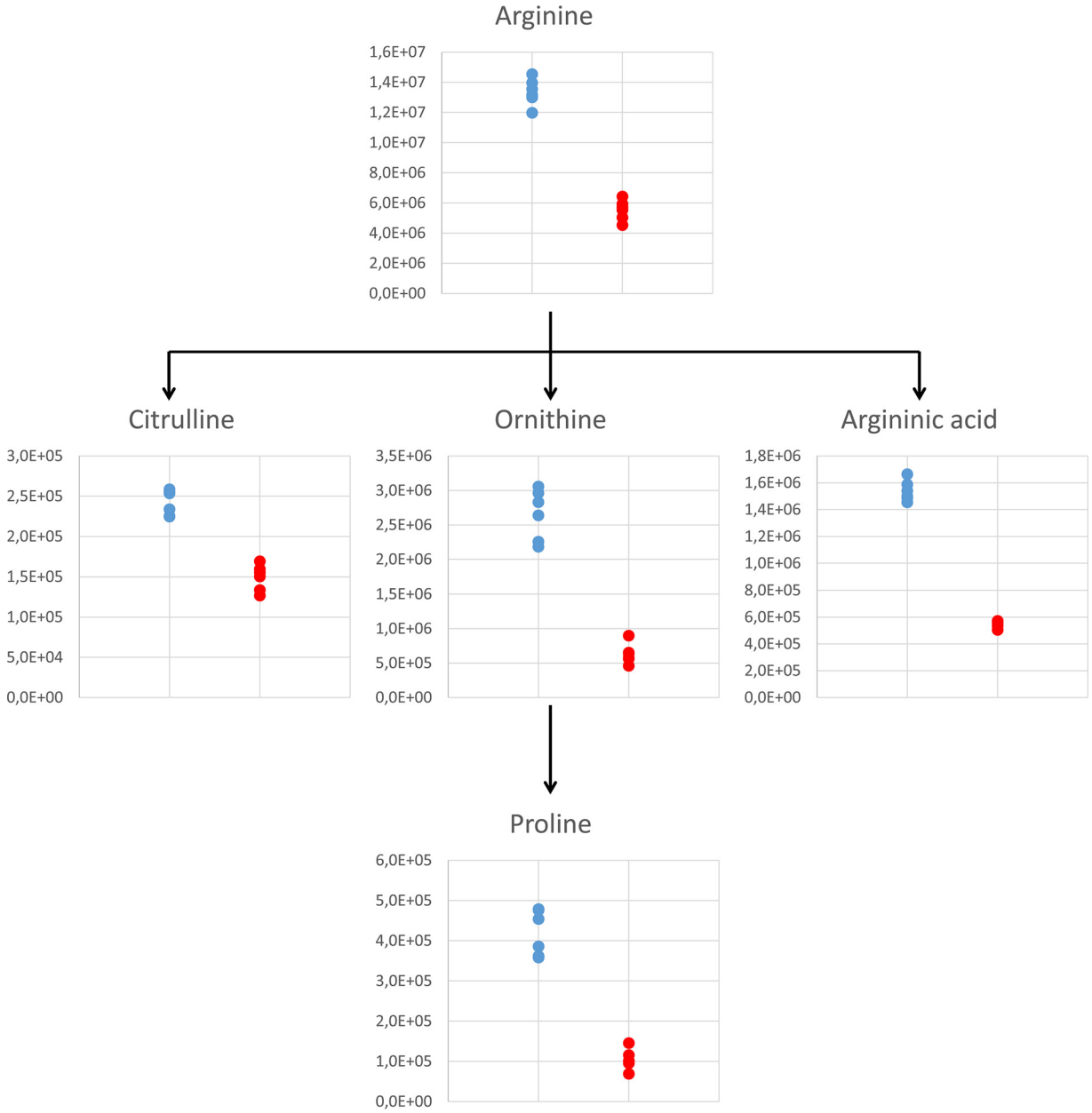

FIG 1 Effect of miltefosine on arginine metabolism observed in *L. donovani* axenic amastigotes after 24 h of exposure at the lower dose of 4.47 μM. Plots show peak area abundances detected in samples: untreated parasites are in blue, and parasites treated with 4.47 μM miltefosine are in red.

sphingosine abundance induced by miltefosine ($P = 2 \times 10^{-6}$) was mirrored by a 3-fold increase in sphinganine ($P = 7 \times 10^{-4}$). All detected ceramides were also substantially increased by 24 h, as shown and detailed in Table S3.

***L. major* promastigotes.** *Leishmania* SL metabolism has been best studied in the promastigote form of *L. major*, where a ΔLCB2 mutant lacking the first enzyme of the biosynthetic pathway, serine palmitoyl transferase, is available (28, 31). The effects of miltefosine in these *L. major* promastigotes were therefore investigated. The efficacy of miltefosine was established against both the ΔLCB2 mutant and wild-type lines; the EC_{50} for the wild type was 6.83 μM, consistent with previous literature (33), while for the mutant, the EC_{50} was three times higher at 21.21 μM. The lipidome of these parasites revealed major differences between the wild-type and ΔLCB2 lines, and the effects of miltefosine were also compared. Lipids identified with marked differences in

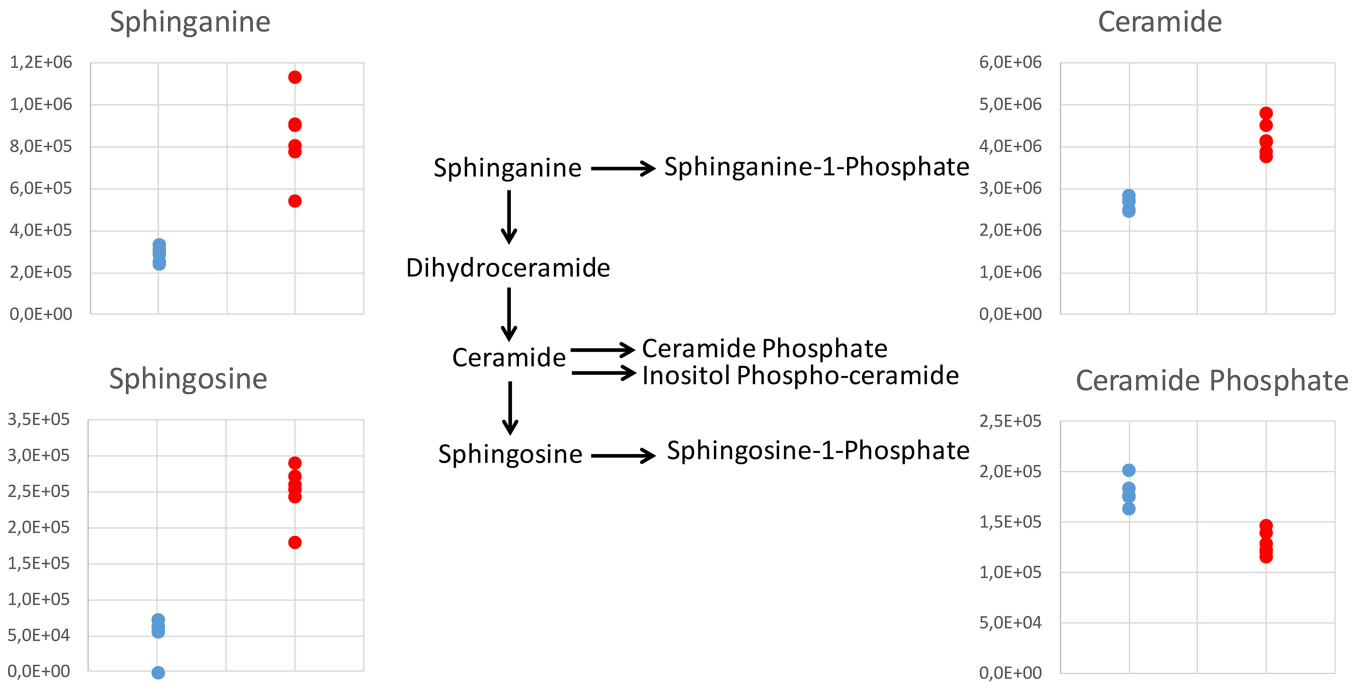

FIG 2 Effect of miltefosine on the SL biosynthetic pathway observed in *L. donovani* axenic amastigotes after 24 h of exposure at the lower dose of 4.47 μM. Plots show peak area abundances for key SLs detected in samples: untreated parasites are in blue, parasites treated with 4.47 μM miltefosine are in red. Sphinganine shown is the C_{16} form, ceramide shown is the 34:1 form, sphingosine shown is the 18:1 form, and ceramide phosphate shown is 26:1 form. Plots show trends representative of all detected SLs of their type. For full list of detected SLs, refer to Table S3.

abundance between any experimental groups compared are detailed in Tables S5 to S7. As in *L. donovani*, miltefosine itself and around 20 other features were detected only in treated samples. Miltefosine was identified in both the wild type and ΔLCB2 mutant, with no significant difference in relative concentration ($P = 0.09$ for the lower dose and $P = 0.45$ at the higher dose). This demonstrated that the 3-fold resistance of the mutant was not due to inhibited import. As in *L. donovani* in this study and as reported in *L. infantum* previously (6), miltefosine caused substantial effects in levels of numerous PLs in *L. major* as well. This reduction may be due to reduced import of PLs or choline or to reduced *de novo* biosynthesis.

The effects of miltefosine on *L. major* SLs were similar to those observed after 24 h of exposure in *L. donovani* amastigotes. Figure 3 shows the fold changes for both doses. As can be seen, some SLs were detected only in *L. donovani* or only in *L. major*. This may be due to species-specific differences and could even be due to differences in the mechanism of each species given that they cause different forms of leishmaniasis (*L. donovani* causing the visceral form and *L. major* the cutaneous form). The *L. major* ΔLCB2 mutants lack most SLs, in accordance with them being devoid of SL biosynthesis. Sphingosine and ceramide (d36:1), however, were detected, indicating that they are acquired from the media. Likewise, SM may also be derived from the media, since there is no evidence that *Leishmania* spp. synthesize SM, although they do possess SMase, which has been shown to be essential in degrading host-derived SM to promote parasite survival, proliferation, and virulence (40). The increase in SLs could indicate a stimulatory effect of miltefosine on biosynthesis or inhibition of a catabolic pathway, with the latter seeming more likely since the mutant also accumulates higher levels of the two SLs detected (SM and ceramide d36:1 upon treatment) (Fig. 3).

As in *L. donovani*, sterols were also increased by treatment in the *L. major* wild type, though not in ΔLCB2 mutants. The identification of sterols poses a particular challenge, since many in the pathway share identical masses. However, using the calculated LogP values, it was possible to identify each based on their elution order in the LC-MS data, as shown in File S2. Figure 4 shows the ergosterol biosynthesis pathway and highlights

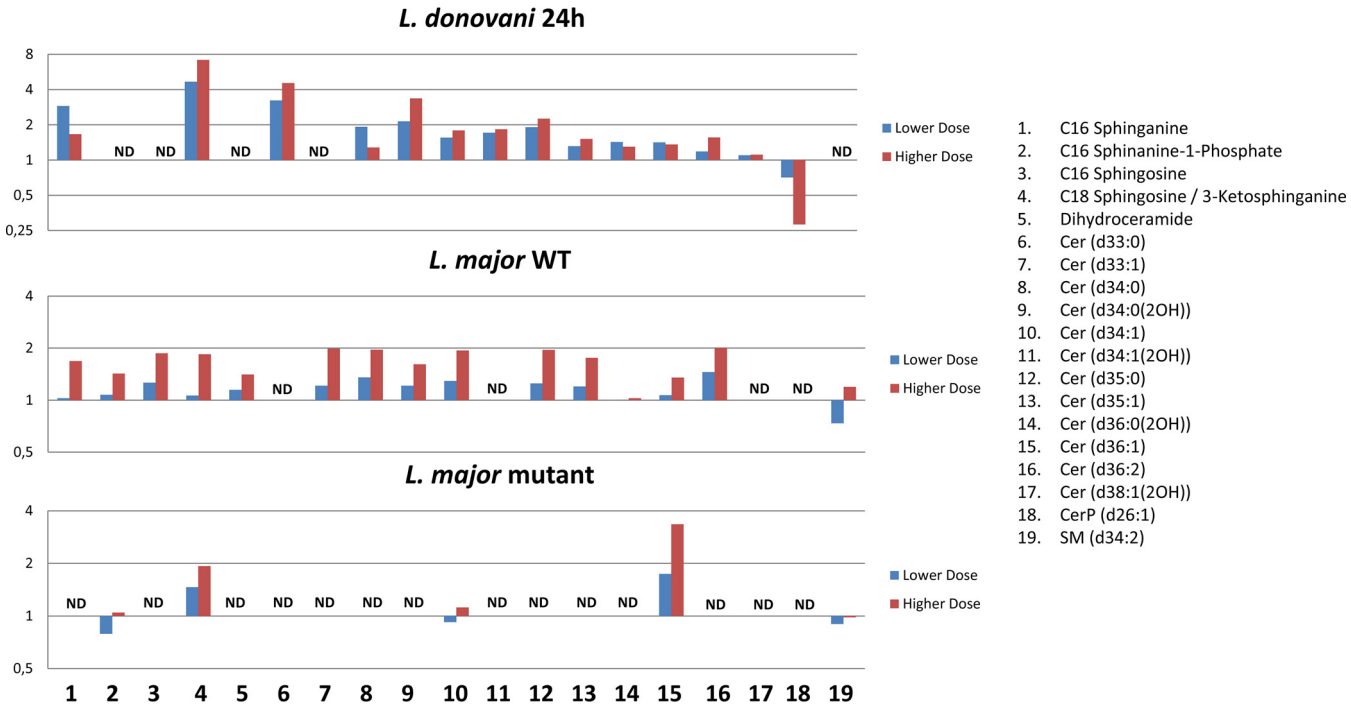

FIG 3 Fold changes in abundance of all SLs detected in *L. donovani* axenic amastigotes and/or *L. major* promastigotes, comparing treated parasites to untreated parasites. Lower-dose and higher-dose data are shown for each, corresponding to 4.47 μM and 13.41 μM, respectively, for *L. donovani* and 10 μM and 30 μM, respectively, for *L. major*. SLs that were not detected in a certain data set are marked with ND, while X denotes complete absence in drug-treated parasites and presence in untreated parasites.

observed increases in *L. donovani* after 5 h (blue arrows) and 24 h (red arrows) of miltefosine exposure and in the *L. major* wild type after 5 h (green arrows) of miltefosine exposure. The trends were the same for both concentrations of the drug, except for fecosterol at the higher dose in *L. donovani*, which was increased, albeit not significantly.

Although sterol differences were not observed with treatment in ΔLCB2 mutants (Table S7), comparison to the untreated wild type revealed dramatic differences in sterol metabolism, particularly with respect to ergosterol and cholesterol. This alteration in sterol composition in the selection of the mutant is particularly noteworthy, since it enables the mutant to survive without SL synthesis, while the change in sterol composition may stabilize membranes in the face of miltefosine treatment, emphasizing the complex interplay between SL and sterol metabolism. As shown in the chromatographic peaks in Fig. 4, ergosterol levels were significantly reduced (approximately halved $P = 5 \times 10^{-14}$) in the ΔLCB2 mutant relative to the wild type, while cholesterol levels were around 3-fold more abundant ($P = 8 \times 10^{-12}$). Cholesterol is probably scavenged in *Leishmania* species (26). Ergosterol was significantly increased with treatment in the wild type and was of much lower abundance in the mutant, which exhibits a 3-fold reduced sensitivity to the drug. 5,7,22,24(28)-Ergostatetraenol, which precedes ergosterol in its synthetic pathway, is also dramatically more abundant in ΔLCB2 mutants than in the wild type, which suggests that the final step in ergosterol synthesis (catalyzed by erg4) is diminished in the mutant. Two further sterols, which share the same mass as ergosterol, 5,7,24(28)-ergostatrienol and 5-dehydroepisterol, were observed in the mutant but were below the limit of detection in the wild type. Their accumulation may also occur due to the reduced production in ergosterol biosynthesis later in the pathway.

The ΔLCB2 *Leishmania* mutants are viable, while the same enzyme is essential to African trypanosomes. This has been proposed to be due to *Leishmania* spp., depending on ergosterol as its primary sterol rather than cholesterol as in *T. brucei* (29).

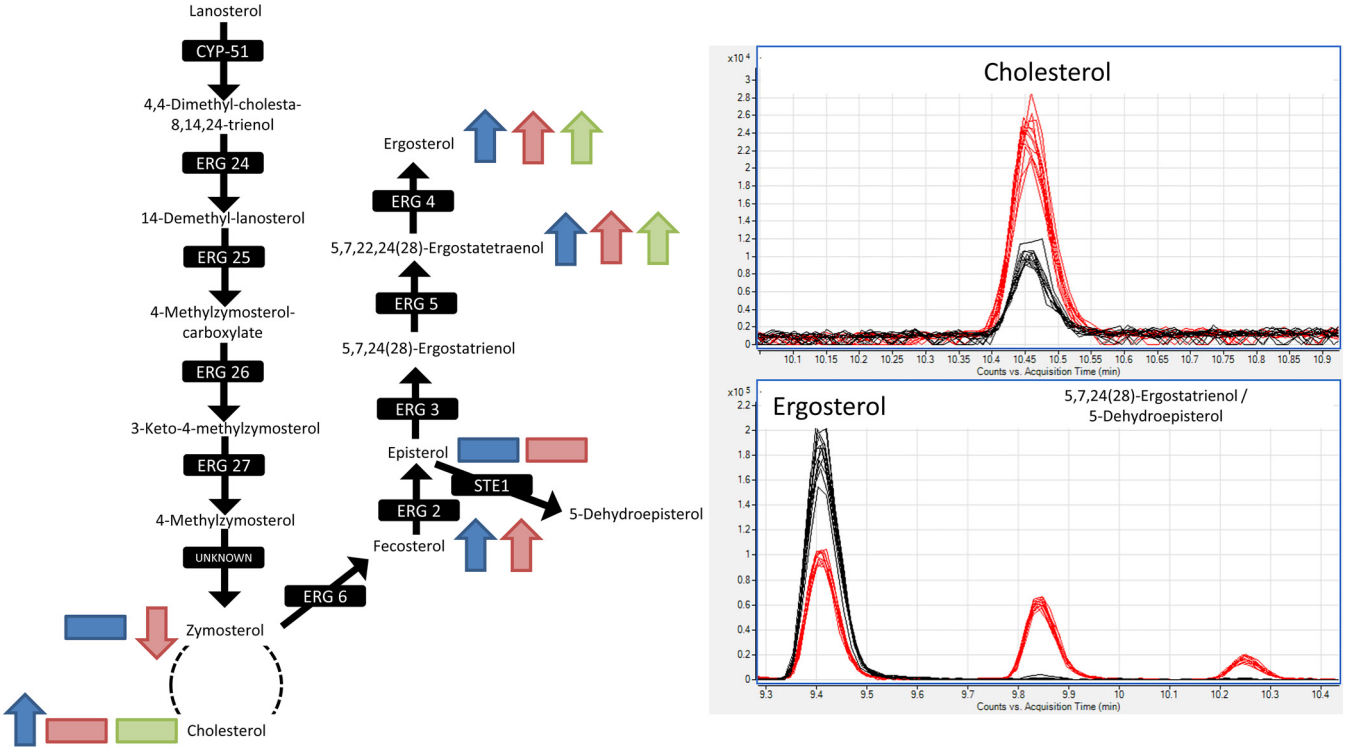

FIG 4 Ergosterol biosynthesis pathway. Sterols that increased, decreased, or were detected but with no change as a response to miltefosine exposure are shown on the pathway (*L. donovani* axenic amastigotes with 5-h drug exposure in blue, *L. donovani* axenic amastigotes with 24-h drug exposure in red, *L. major* wild-type promastigotes in green). In all cases, trends were seen for both low and high concentrations of miltefosine treatment. Chromatographic peaks shown for ergosterol, cholesterol, 5,7,24(28)-ergostatrienol, and 5-dehydroepisterol in *L. major* wild type (black trace) and ΔLCB2 mutants (red trace) to highlight the differences in sterol profiles between them. 5,7,24(28)-Ergostatrienol and 5-dehydroepisterol share the same logP, and therefore, it is not possible to distinguish to which peak (9.8 to 9.9 min or 10.2 to 10.3 min) these sterols correspond.

However, since the ΔLCB2 mutant exhibits much higher cholesterol and lower ergosterol concentrations than the wild type, the simplistic view of changes in cholesterol versus ergosterol appears to be inadequate to explain the essential nature of SL synthesis in *T. brucei*. Though the magnitude of this sterol balance is not as severe as in *T. brucei*, the retained viability in the absence of SL synthesis is likely to be due to other reasons. As observed in the *L. major* ΔLCB2 mutants, ergosterol reduction has been reported in a strain of *L. infantum* resistant to 200 μM miltefosine compared to in the wild type (41), although the mechanism of resistance was reported to be associated with mutations in the miltefosine transporter. In *L. donovani* promastigotes, membrane sterol depletion has been correlated with reduced sensitivity to miltefosine (42). In that study, the authors tested a hypothesis that lipid rafts could be involved in miltefosine action by destabilizing these microdomains through the depletion of sterols using either methyl-β-cyclodextrin (MCD) or cholesterol oxidase (CH-OX). Sterol depletion showed no significant effects on the viability of either the wild type or mutant; however, MCD treatment significantly decreased the susceptibility of the wild type to miltefosine (around 2-fold), although CH-OX depletion caused no significant effect. Since MCD has less specificity in sterol extraction than CH-OX, MCD is likely to deplete ergosterol and other sterols in addition to cholesterol, pointing to a possible link between ergosterol depletion and reduced miltefosine activity. Increases in ergosterol in *L. donovani* and *L. major* (wild type) coordinated with an increase in SLs reported here may also point toward a function of lipid microdomain complexes of sterols and SLs (27, 29, 42) in the effects of miltefosine on the parasites. Apoptosis has been proposed as an effect of miltefosine in tumor cells relating to lipid microdomains (43–45). Though the existence of apoptosis in *Leishmania* spp. has been challenged (46), various indications point to miltefosine inducing an apoptosis-like death in *L. donovani* promastigotes (16). It is

clear that miltefosine treatment causes profound changes to the lipid contents of *Leishmania* amastigotes and promastigotes, and that alterations in lipid composition, such as a loss of SL biosynthesis and an accompanying change in sterol metabolism, impact this action of the drug.

Conclusion. A robust platform offering broad coverage of *Leishmania* metabolites using two complementary techniques was developed to study the miltefosine MoA. In addition to revealing the effects of miltefosine on internal metabolites and possible interference with membrane transport, many lipid species were shown to be perturbed by treatment, and importantly, SLs and sterols were found to increase. These findings, initially observed in *L. donovani* axenic amastigotes, were confirmed in *L. major* promastigotes for which a defined ΔLCB2 mutant, devoid of SL biosynthesis, was available. These mutant parasites lacked SLs, other than those derived from the culture medium, and sterol metabolism was drastically altered compared with the wild type. This lipidomic remodelling was associated with a 3-fold reduction in sensitivity to miltefosine. Coupled with the observation that sterol concentrations increase when both *L. major* and *L. donovani* wild-type parasites were exposed to miltefosine, a major role for these lipids in miltefosine resistance and, perhaps MoA, is indicated.

MATERIALS AND METHODS

Experimental design. In order to define the optimal protocol for sampling/quenching/extracting/analyzing metabolites from *L. donovani* axenic amastigotes, a two-stage experiment was designed that (i) allowed a reproducible global profile of metabolites to be obtained and (ii) allowed the execution of the optimized protocol in the exploration of miltefosine MoA. It was necessary to optimize parasite seeding densities and harvesting numbers to work with 5-h and 24-h time points to obtain sufficient biomass for metabolomics analyses, while also ensuring log-phase growth (metabolic steady state) in parasites at the time of harvesting. Parasites were always seeded from log-phase cultures to minimize lag phase (particularly important at 5 h). Optimal seeding densities were determined to be 6.67×10^6 parasites/ml for samples to be harvested at 5 h and 1.33×10^6 parasites/ml for samples to be harvested at 24 h. Details of the method development are given in full in the supplemental material.

Chemicals and reagents. The axenic culture medium used in all experiments was prepared from one batch prepared "in-house" as described by Peña et al. (2). The culture medium used for the *L. major* wild type was Schneider's *Drosophila* medium (Sigma-Aldrich) supplemented with heat-inactivated fetal bovine serum (15%). All methanol used was high-performance liquid chromatography (HPLC) grade, and formic acid was analytical grade. These chemicals, in addition to formaldehyde solution and phosphate-buffered saline (PBS), were purchased from Sigma-Aldrich. Ultrapure water was obtained using a Milli-Q Plus 185 system (Millipore, Billerica, MA, USA).

Sample collection and quenching of metabolism. *L. donovani* strain 1S2D (WHO designation: MHOM/SD/62/1S-CL2D) (47) was cultured by cycling between promastigotes and axenic amastigotes using protocols from prior work (2). Briefly, the promastigote form was grown at 29°C, and amastigote forms were grown at 37°C with 5% CO_2 in different media adapted by De Rycker et al. (48). For experiments with miltefosine, three T75 flasks were prepared (with 30 ml of culture at the appropriate densities for 5 h or 24 h, as described above) for each condition: nontreated parasites, parasites treated with the lower dose of miltefosine (4.47 μM), and parasites treated with the higher dose of miltefosine (13.41 μM).

At the time of sample harvesting, culture from each flask was divided equally into two 15-ml Falcon tubes, resulting in six replicate samples for each condition. Before the division, 50 μl of each culture was collected into Eppendorf tubes to which 50 μl formaldehyde was added, and samples were stored at 4°C to be counted later in order to record the exact number of parasites from each flask at the time of harvesting. At the time of harvesting and throughout the subsequent processes, samples were maintained at 4°C.

After the collection of culture, each sample was centrifuged at 1,500 $\times$ *g* at 4°C for 15 min, after which medium was decanted and parasites were washed in 2 ml PBS (maintained at 4°C); then, samples were transferred to 2-ml Eppendorf tubes. From each sample, 10 μl was taken, fixed with 10 μl of formaldehyde, and stored at 4°C to be counted later in order to record the exact number of parasites in each sample immediately before quenching. Samples were subsequently centrifuged at 1,500 $\times$ *g* at 4°C for 15 min, PBS was decanted, and 200 μl ice-cold methanol was added to each sample; samples were immediately stored at −80°C until extraction and metabolomics analysis. Figure S1 shows the workflow for the developed method for sampling.

Leishmania major parasites (MHOM/IL/81/Friedlin; FV1 strain) and a mutant in which the catalytic subunit of serine palmitoyltransferase had been deleted by homologous recombination (ΔLCB2) (31) were cultured as log-phase promastigotes at 26°C. Samples were prepared for metabolomics as described for *L. donovani* with the appropriate miltefosine doses described above, except 10 μM and 30 μM were used for the lower and higher doses of miltefosine, respectively.

Metabolite extraction. Extraction blanks were prepared following all stages of extraction. On the day of analyses, metabolites were extracted and supernatants analyzed by LC-MS (and for all *L. donovani* samples in CE-MS as well). Samples were prepared by first evaporating extracts to dryness using a speed

vacuum concentrator (Eppendorf, Hamburg, Germany), after which 200 mg of 425- to 600-μm acid-washed glass beads was added. Then to *L. donovani* samples, 575 μl of 100% methanol was added, before which samples were vortexed for 10 min and placed in a tissue lyzer for 30 min at 50 Hz. Finally, samples were centrifuged at 16,000 $\times$ *g* at 4°C for 10 min, and 80 μl of the resulting supernatants was collected into LC-MS vials to be analyzed directly. To the remaining samples (for CE-MS), 165 μl of water was added; they were vortexed for 30 min, centrifuged at 16,000 $\times$ *g* at 4°C for 10 min, evaporated to dryness, and resuspended in 100 μl of water containing 0.2 M methionine sulfone (internal standard), after which 0.1 mM formic acid was added to each. Quality control (QC) samples for LC-MS and CE-MS were prepared by collecting 10 μl from each sample into a single pool. For *L. major*, only LC-MS extracts were prepared; therefore, after evaporation, 120 mg of 425- to 600-μm acid-washed glass beads and 350 μl methanol were added for extraction, and 270 μl of the resulting supernatants following extraction was collected into LC-MS vials to be analyzed directly, from which 30 μl was subtracted from each into a pool.

Analysis of extracts by LC-MS and CE-MS. For each analysis, extraction blanks were injected at the start of the analysis, followed by eight injections of the QC sample in order to ensure system stability; samples were then analyzed in random order, with the QC sample injected after every sixth sample until the end of the analysis. All instrumentation was from Agilent Technologies. For LC-MS, a 1290 infinity LC equipped with reverse-phase column (Zorbax Extend C_{18}, 50 by 2.1 mm, 3 μm; Agilent) was coupled to a 6550 Q-TOF MS with electrospray ionization source and operated in both positive and negative mode. For CE-MS, the instrument consisted of a 7100 CE coupled to a 6224 TOF MS operated in positive mode. Details of the analytical procedures based on previously published methods (49, 50) are given in the supplemental material.

Data analysis and feature identification. Data from both platforms were processed using recursive analysis in MassHunter Profinder (B.06.00; Agilent) software, as detailed in the supplemental material. Data were reprocessed considering ions such as $[M+H]^+$ and $[M+Na]^+$, with neutral water loss and a maximum permitted charge state that was double. Alignment was performed based on *m/z* and retention time (RT) similarities within the samples. The parameters applied were 1% for the RT window and 20 ppm for mass tolerance.

Data treatment consisted of filtering based on quality, following the same procedure for each data set (*L. donovani*, LC-MS positive-ion mode, LC-MS negative-ion mode, CE-MS positive-ion mode; *L. major*, LC-MS positive-ion mode, and LC-MS negative-ion mode). Data were filtered based on quality using a quality assurance procedure described previously (QA+) (51). This involved retaining features present in QC samples at a rate of 80% or absent in QC samples (defined as presence <20%). For features present in QC samples, only those with relative standard deviations (RSDs) of <30% were kept, and for those that were absent, the RSD was not calculated. Then, for each comparison separately (5 h, 24 h, wild type, or ΔLCB2 mutant), features were further filtered to keep only those present in at least five out of six of the replicates from one of the groups simultaneously compared (resulting in a slightly different but relevant data set for each comparison).

First, *L. donovani* multivariate analysis was employed to observe the stability in each analysis (LC-MS in positive- and negative-ionization modes or CE-MS) as a whole and then for each time point separately to investigate the effect of the drug on the parasite metabolome. To probe specific questions on the effect of miltefosine at different time points or doses, fold changes and *P* values were calculated in order to assess the degree of significance of any difference observed in the raw data.

All significantly different metabolite features between untreated and treated parasites at any dose, as determined by a *P* value of <0.05 (Student's two-tailed *t* test, $n = 6$ per group) and a fold change of $\pm$1.5, were identified. Identification was performed by searching *m/z* against Metlin (http://metlin.scripps.edu) and Lipid Maps (http://lipidMAPS.org), considering the same adducts as those described for data reprocessing. Annotations were assigned to *m/z* values for metabolite features taking into consideration (i) mass accuracy (maximum mass error, 10 ppm), (ii) isotopic pattern distribution, (iii) the possibility of cation and anion formation, and (iv) adduct formation. This method of enhanced annotation was based on our previously published work (49). Where possible, identifications were compared by retention time order to standards analyzed in-house. For CE-MS, definitive identifications were made for a number of metabolites through an analysis of authentic standards analyzed under the same conditions as the experiment, whereby samples were analyzed again followed by the same samples spiked with authentic standards to prove the identity.

All data analyzed during this study are included in this article and in the tables in the supplemental material.

SUPPLEMENTAL MATERIAL

Supplemental material for this article may be found at https://doi.org/10.1128/AAC.02095-17.

SUPPLEMENTAL FILE 1, PDF file, 2.0 MB.

SUPPLEMENTAL FILE 2, XLSX file, 0.2 MB.

ACKNOWLEDGMENTS

We acknowledge funding provided by the Tres Cantos Open Lab Foundation (TCOLF; program code TC132). In addition, E.G.A., J.G., V.A.-H., Á.L.-G., and C.B. acknowledge the Spanish Ministerio de Economia y Competitividad for funding

(grant CTQ2014-55279-R). M.P.B. is funded by a core grant to the Wellcome Centre for Molecular Parasitology (104111/Z/14/Z), and A.Q.I.A., A.J.M., and P.W.D. acknowledge funding from the BBSRC (grant BB/M024156/1), MRC (grant MR/P027989/1), and Government of Iraq.

REFERENCES

1. Kim D-H, Creek DJ. 2015. What role can metabolomics play in the discovery and development of new medicines for infectious diseases? Bioanalysis 7:629–631. https://doi.org/10.4155/bio.15.5.
2. Peña I, Pilar Manzano M, Cantizani J, Kessler A, Alonso-Padilla J, Bardera AI, Alvarez E, Colmenarejo G, Cotillo I, Roquero I, de Dios-Anton F, Barroso V, Rodriguez A, Gray DW, Navarro M, Kumar V, Sherstnev A, Drewry DH, Brown JR, Fiandor JM, Julio Martin J. 2015. New compound sets identified from high throughput phenotypic screening against three kinetoplastid parasites: an open resource. Sci Rep 5:8771. https://doi.org/10.1038/srep08771.
3. Pedrique B, Strub-Wourgaft N, Some C, Olliaro P, Trouiller P, Ford N, Pécoul B, Bradol JH. 2013. The drug and vaccine landscape for neglected diseases (2000–11): a systematic assessment. Lancet Glob Health 1:371–379.
4. Canuto GAB, Castilho-Martins EA, Tavares MF, Rivas L, Barbas C, Lopez-Gonzalvez A. 2014. Multi-analytical platform metabolomic approach to study miltefosine mechanism of action and resistance in Leishmania. Anal Bioanal Chem 406:3459–3476. https://doi.org/10.1007/s00216-014-7772-1.
5. Saunders EC, Ng WW, Chambers JM, Ng M, Naderer T, Kro JO, Likic VA, McConville MJ. 2011. Isotopomer profiling of Leishmania mexicana promastigotes reveals important roles for succinate fermentation and aspartate uptake in tricarboxylic acid cycle (TCA) anaplerosis, glutamate synthesis, and growth. J Biol Chem 286:27706–27717. https://doi.org/10.1074/jbc.M110.213553.
6. Vincent IM, Weidt S, Rivas L, Burgess K, Smith TK, Ouellette M. 2014. Untargeted metabolomic analysis of miltefosine action in *Leishmania infantum* reveals changes to the internal lipid metabolism. Int J Parasitol Drugs Drug Resist 4:20–27. https://doi.org/10.1016/j.ijpddr.2013.11.002.
7. Zheng L, T'Kind R, Decuypere S, von Freyend SJ, Coombs GH, Watson DG. 2010. Profiling of lipids in *Leishmania donovani* using hydrophilic interaction chromatography in combination with Fourier transform mass spectrometry. Rapid Commun Mass Spectrom 24:2074–2082. https://doi.org/10.1002/rcm.4618.
8. Rojo D, Canuto GAB, Castilho-Martins EA, Tavares MFM, Barbas C, López-González Á, Rivas L. 2015. A multiplatform metabolomic approach to the basis of antimonial action and resistance in *Leishmania infantum*. PLoS One 10:e0130675. https://doi.org/10.1371/journal.pone.0130675.
9. Canuto GAB, Castilho-Martins EA, Tavares M, López-González Á, Rivas L, Barbas C. 2012. CE-ESI-MS metabolic fingerprinting of *Leishmania* resistance to antimony treatment. Electrophoresis 33:1901–1910. https://doi.org/10.1002/elps.201200007.
10. Castilho-Martins EA, Canuto GAB, Muxel SM, da Silva MFL, Floeter-Winter LM, Del Aguila C, López-González Á, Barbas C. 2015. Capillary electrophoresis reveals polyamine metabolism modulation in *Leishmania* (*Leishmania*) *amazonensis* wild-type and arginase-knockout mutants under arginine starvation. Electrophoresis 36:2314–2323. https://doi.org/10.1002/elps.201500114.
11. Alves-Ferreira EVC, Toledo JS, De Oliveira AHC, Ferreira TR, Ruy PC, Pinzan CF, Santos RF, Boaventura V, Rojo D, López-González Á, Rosa JC, Barbas C, Barral-Netto M, Barral A, Cruz AK. 2015. Differential gene expression and infection profiles of cutaneous and mucosal *Leishmania braziliensis* isolates from the same patient. PLoS Negl Trop Dis 9:e0004018. https://doi.org/10.1371/journal.pntd.0004018.
12. Scheltema RA, Decuypere S, T'kindt R, Dujardin J-C, Coombs GH, Breitling R. 2010. The potential of metabolomics for *Leishmania* research in the post-genomics era. Parasitology 137:1291–1302. https://doi.org/10.1017/S0031182009992022.
13. t'Kindt R, Scheltema RA, Jankevics A, Brunker K, Rijal S, Dujardin JC, Breitling R, Watson DG, Coombs GH, Decuypere S. 2010. Metabolomics to unveil and understand phenotypic diversity between pathogen populations. PLoS Negl Trop Dis 4:e904. https://doi.org/10.1371/journal.pntd.0000904.
14. Saunders EC, Ng WW, Kloehn J, Chambers JM, Ng M, McConville MJ. 2014. Induction of a stringent metabolic response in intracellular stages of *Leishmania mexicana* leads to increased dependence on mitochondrial metabolism. PLoS Pathog 10: e1003888. https://doi.org/10.1371/journal.ppat.1003888.
15. Moreira W, Leprohon P, Ouellette M. 2011. Tolerance to drug-induced cell death favours the acquisition of multidrug resistance in *Leishmania*. Cell Death Dis 2:e201. https://doi.org/10.1038/cddis.2011.83.
16. Paris C, Loiseau PM, Bories C, Bréard J. 2004. Miltefosine induces apoptosis-like death in *Leishmania donovani* promastigotes. Antimicrob Agents Chemother 48:852–859. https://doi.org/10.1128/AAC.48.3.852-859.2004.
17. Inbar E, Canepa GE, Carrillo C, Glaser F, Grotemeyer MS, Rentsch D, Zilberstein D, Pereira CA. 2012. Lysine transporters in human trypanosomatid pathogens. Amino Acids 42:347–360. https://doi.org/10.1007/s00726-010-0812-z.
18. Darlyuk I, Goldman A, Roberts SC, Ullmarr B, Rentsch D, Zilberstein D. 2009. Arginine homeostasis and transport in the human pathogen *Leishmania donovani*. J Biol Chem 284:19800–19807. https://doi.org/10.1074/jbc.M901066200.
19. Pérez-Victoria FJ, Sánchez-Cañete MP, Castanys S, Gamarro F. 2006. Phospholipid translocation and miltefosine potency require both *L. donovani* miltefosine transporter and the new protein LdRos3 in *Leishmania* parasites. J Biol Chem 281:23766–23775. https://doi.org/10.1074/jbc.M605214200.
20. Gazanion É, Fernández-Prada C, Papadopoulou B, Leprohon P, Ouellette M. 2016. Cos-Seq for high-throughput identification of drug target and resistance mechanisms in the protozoan parasite *Leishmania*. Proc Natl Acad Sci U S A. 113:E3012–E3021.
21. Zufferey R, Mamoun CB. 2002. Choline transport in Leishmania major promastigotes and its inhibition by choline and phosphocholine analogs. Mol Biochem Parasitol 125:127–134. https://doi.org/10.1016/S0166-6851(02)00220-7.
22. Rakotomanga M, Blanc S, Gaudin K, Chaminade P, Loiseau PM. 2007. Miltefosine affects lipid metabolism in Leishmania donovani promastigotes. Antimicrob Agents Chemother 51:1425–1430. https://doi.org/10.1128/AAC.01123-06.
23. Rakotomanga M, Loiseau PM, Saint-Pierre-Chazalet M. 2004. Hexadecylphosphocholine interaction with lipid monolayers. Biochim Biophys Acta 1661:212–218. https://doi.org/10.1016/j.bbamem.2004.01.010.
24. Lux H, Heise N, Klenner T, Hart D, Opperdoes FR. 2000. Ether-lipid (alkyl-phospholipid) metabolism and the mechanism of action of ether-lipid analogues in Leishmania. Mol Biochem Parasitol 111:1–14. https://doi.org/10.1016/S0166-6851(00)00278-4.
25. Wassef MK, Fioretti TB, Dwyer DM. 1985. Lipid analyses of isolated surface membranes of Leishmania donovani promastigotes. Lipids 20:108–115. https://doi.org/10.1007/BF02534216.
26. Yao C, Wilson ME. 2016. Dynamics of sterol synthesis during development of Leishmania spp. parasites to their virulent form. Parasit Vectors 9:200. https://doi.org/10.1186/s13071-016-1470-0.
27. Denny PW, Smith DF. 2004. Rafts and sphingolipid biosynthesis in the kinetoplastid parasitic protozoa. Mol Microbiol 53:725–733. https://doi.org/10.1111/j.1365-2958.2004.04208.x.
28. Zhang K, Pompey JM, Hsu F-F, Key P, Bandhuvula P, Saba JD, Turk J, Beverley SM. 2007. Redirection of sphingolipid metabolism toward *de novo* synthesis of ethanolamine in *Leishmania*. EMBO J 26:1094–1104. https://doi.org/10.1038/sj.emboj.7601565.
29. Zhang K, Beverley SM. 2010. Phospholipid and sphingolipid metabolism in Leishmania. Mol Biochem Parasitol 170:55. https://doi.org/10.1016/j.molbiopara.2009.12.004.
30. Ivens AC, Peacock CS, Worthey EA, Murphy L, Berriman M, Sisk E, Rajandream M, Adlem E, Anupama A, Apostolou Z, Attipoe P, Bason N, Beck A, Beverley SM, Bianchettin G, Borzym K, Bothe G, Bruschi CV, Collins M, Cadag E, Ciarloni L, Clayton C, Coulson RMR, Cronin A, Cruz AK, Robert M, De Gaudenzi J, Dobson DE, Duesterhoeft A, Fosker N, Frasch AC, Fraser A, Fuchs M, Goble A, Goffeau A, Harris D, Hertz-Fowler C, Horn D, Huang Y, Klages S, Knights A, Kube M, Matthews K, Michaeli S, Mottram JC, Müller-Auer S, Munden H, Nelson S, Norbertczak H, Oliver K, et al.

2006. The genome of the kinetoplastid parasite, Leishmania major. Science 309:436–442. https://doi.org/10.1126/science.1112680.
31. Denny PW, Goulding D, Ferguson MAJ, Smith DF. 2004. Sphingolipid-free Leishmania are defective in membrane trafficking, differentiation and infectivity. Mol Microbiol 52:313–327. https://doi.org/10.1111/j.1365-2958.2003.03975.x.
32. Fridberg A, Olson CL, Nakayasu ES, Tyler KM, Almeida IC, Engman DM. 2008. Sphingolipid synthesis is necessary for kinetoplast segregation and cytokinesis in Trypanosoma brucei. J Cell Sci 121:522–535. https://doi.org/10.1242/jcs.016741.
33. Escobar P, Matu S, Marques C, Croft SL. 2002. Sensitivities of Leishmania species to hexadecylphosphocholine (miltefosine), ET-18-OCH_3 (edelfosine) and amphotericin B. Acta Trop 81:151–157. https://doi.org/10.1016/S0001-706X(01)00197-8.
34. Goldman-Pinkovich A, Balno C, Strasser R, Zeituni-Molad M, Bendelak K, Rentsch D, Ephros M, Wiese M, Jardim A, Myler PJ, Zilberstein D. 2016. An arginine deprivation response pathway is induced in Leishmania during macrophage invasion. PLoS Pathog 12:1–18. https://doi.org/10.1371/journal.ppat.1005494.
35. Castilho-Martins EA, Laranjeira da Silva MF, dos Santos MG, Muxel SM, Floeter-Winter LM. 2011. Axenic leishmania amazonensis promastigotes sense both the external and internal arginine pool distinctly regulating the two transporter-coding genes. PLoS One 6:e27818. https://doi.org/10.1371/journal.pone.0027818.
36. Westrop GD, Williams RAM, Wang L, Zhang T, Watson DG, Silva AM, Coombs GH. 2015. Metabolomic analyses of Leishmania reveal multiple species differences and large differences in amino acid metabolism. PLoS One 10:e0136891. https://doi.org/10.1371/journal.pone.0136891.
37. Silva AM, Cordeiro-da-Silva A, Coombs GH. 2011. Metabolic variation during development in culture of leishmania donovani promastigotes. PLoS Negl Trop Dis 5:e1451. https://doi.org/10.1371/journal.pntd.0001451.
38. Shaw CD, Lonchamp J, Downing T, Imamura H, Freeman TM, Cotton JA, Sanders M, Blackburn G, Dujardin JC, Rijal S, Khanal B, Illingworth CJR, Coombs GH, Carter KC. 2016. *In vitro* selection of miltefosine resistance in promastigotes of *Leishmania donovani* from Nepal: genomic and metabolomic characterization. Mol Microbiol 99:1134–1148. https://doi.org/10.1111/mmi.13291.
39. Imbert L, Ramos RG, Libong D, Abreu S, Loiseau PM, Chaminade P. 2012. Identification of phospholipid species affected by miltefosine action in Leishmania donovani cultures using LC-ELSD, LC-ESI/MS, and multivariate data analysis. Anal Bioanal Chem 402:1169–1182. https://doi.org/10.1007/s00216-011-5520-3.
40. Zhang O, Wilson MC, Xu W, Hsu FF, Turk J, Kuhlmann FM, Wang Y, Soong L, Key P, Beverley SM, Zhang K. 2009. Degradation of host sphingomyelin is essential for Leishmania virulence. PLoS Pathog 5.
41. Fernandez-Prada C, Vincent IM, Brotherton M-C, Roberts M, Roy G, Rivas L, Leprohon P, Smith TK, Ouellette M. 2016. Different mutations in a P-type ATPase transporter in Leishmania parasites are associated with cross-resistance to two leading drugs by distinct mechanisms. PLoS Negl Trop Dis 10:e0005171. https://doi.org/10.1371/journal.pntd.0005171.
42. Saint-Pierre-Chazalet M, Ben Brahim M, Le Moyec L, Bories C, Rakotomanga M, Loiseau PM. 2009. Membrane sterol depletion impairs miltefosine action in wild-type and miltefosine-resistant Leishmania donovani promastigotes. J Antimicrob Chemother 64:993–1001. https://doi.org/10.1093/jac/dkp321.
43. Henke J, Engelmann J, Flogel U, Pfeuffer J, Kutscher B, Nossner G, Engel J, Voegeli R, Leibfritz D. 1998. Apoptotic effects of hexadecylphosphocholine on resistant and nonresistant cells monitored by NMR spectroscopy. Drugs Today 34:37–50. https://doi.org/10.1358/dot.1998.34.1.485199.
44. Ruiter GA, Verheij M, Zerp SF, van Blitterswijk WJ. 2001. Alkyl-lysophospholipids as anticancer agents and enhancers of radiation-induced apoptosis. Int J Radiat Oncol Biol Phys 49:415–419. https://doi.org/10.1016/S0360-3016(00)01476-0.
45. Rybczynska M, Spitaler M, Knebel NG, Boeck G, Grunicke H, Hofmann J. 2001. Effects of miltefosine on various biochemical parameters in a panel of tumor cell lines with different sensitivities. Biochem Pharmacol 62:765–772. https://doi.org/10.1016/S0006-2952(01)00715-8.
46. Proto WR, Coombs GH, Mottram JC. 2012. Cell death in parasitic protozoa: regulated or incidental? Nat Rev Microbiol 11:58–66. https://doi.org/10.1038/nrmicro2929.
47. Dwyer DM. 1976. Antibody-induced modulation of Leishmania donovani surface membrane antigens. J Immunol 117:2081–2091.
48. De Rycker M, Hallyburton I, Thomas J, Campbell L, Wyllie S, Joshi D, Cameron S, Gilbert IH, Wyatt PG, Frearson JA, Fairlamb AH, Gray DW. 2013. Comparison of a high-throughput high-content intracellular *Leishmania donovani* assay with an axenic amastigote assay. Antimicrob Agents Chemother 57:2913–2922. https://doi.org/10.1128/AAC.02398-12.
49. Godzien J, Ciborowski M, Armitage EG, Jorge I, Camafeita E, Burillo E, Martin-Ventura JL, Rupérez FJ, Vázquez J, Barbas C. 2016. A single in-vial dual extraction strategy for the simultaneous lipidomics and proteomics analysis of HDL and LDL fractions. J Proteome Res 15:1762–1775. https://doi.org/10.1021/acs.jproteome.5b00898.
50. Godzien J, Armitage EG, Angulo S, Martinez-Alcazar MP, Alonso-Herranz V, Otero A, Lopez-Gonzalvez A, Barbas C. 2015. In-source fragmentation and correlation analysis as tools for metabolite identification exemplified with CE-TOF untargeted metabolomics. Electrophoresis 36:2188–2195. https://doi.org/10.1002/elps.201500016.
51. Godzien J, Alonso-Herranz V, Barbas C, Armitage EG. 2014. Controlling the quality of metabolomics data: new strategies to get the best out of the QC sample. Metabolomics 11:518–528. https://doi.org/10.1007/s11306-014-0712-4.